

Article

Sequential Events in the Irreversible Thermal Denaturation of Human Brain-Type Creatine Kinase by Spectroscopic Methods

Yan-Song Gao, Jing-Tan Su and Yong-Bin Yan *

State Key Laboratory of Biomembrane and Membrane Biotechnology, School of Life Sciences, Tsinghua University, Beijing 100084, China

* Author to whom correspondence should be addressed; E-Mail: ybyan@tsinghua.edu.cn; Tel.: +86-10-627-834-77; Fax: +86-10-627-715-97.

Received: 21 May 2010; in revised form: 9 June 2010 / Accepted: 18 June 2010 /

Published: 25 June 2010

Abstract: The non-cooperative or sequential events which occur during protein thermal denaturation are closely correlated with protein folding, stability, and physiological functions. In this research, the sequential events of human brain-type creatine kinase (hBBCK) thermal denaturation were studied by differential scanning calorimetry (DSC), CD, and intrinsic fluorescence spectroscopy. DSC experiments revealed that the thermal denaturation of hBBCK was calorimetrically irreversible. The existence of several endothermic peaks suggested that the denaturation involved stepwise conformational changes, which were further verified by the discrepancy in the transition curves obtained from various spectroscopic probes. During heating, the disruption of the active site structure occurred prior to the secondary and tertiary structural changes. The thermal unfolding and aggregation of hBBCK was found to occur through sequential events. This is quite different from that of muscle-type CK (MMCK). The results herein suggest that BBCK and MMCK undergo quite dissimilar thermal unfolding pathways, although they are highly conserved in the primary and tertiary structures. A minor difference in structure might endow the isoenzymes dissimilar local stabilities in structure, which further contribute to isoenzyme-specific thermal stabilities.

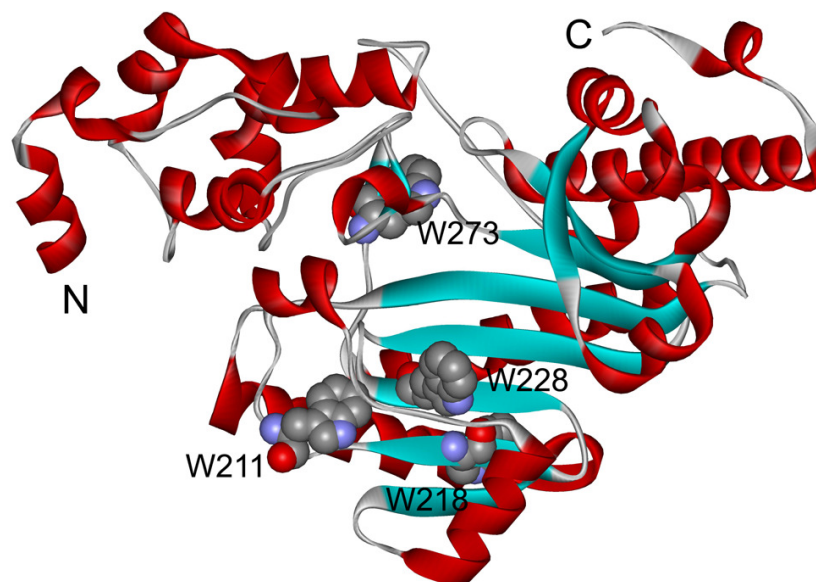
Keywords: differential scanning calorimetry; human brain-type creatine kinase; intrinsic fluorescence; stepwise transitions; thermal denaturation

1. Introduction

When denatured by chemical denaturants, the unfolding of small single-domain proteins is generally a “all” or “none” two-state process, while that of large multimeric or multi-domain proteins is usually a much more complex process that involves a hierarchy of structural transitions [1,2]. As for thermal denaturation, it is traditionally demonstrated by a two-state model for most proteins. The pioneering work by Sherraga and his co-authors has indicated that the thermal unfolding of bovine pancreatic ribonuclease A is a multi-step process, with a sequential melting of protein subdomains or segments [3-6]. Since then, the sequential events in protein thermal unfolding have been characterized in some model proteins by resolution-enhancing spectroscopic techniques, such as two-dimensional correlation spectroscopy [7-20]. The identification of transitions around body temperature suggests that stepwise thermal unfolding may not only play a role in protein thermal stability, but also correlate with the physiological functions of proteins [19-22].

Creatine kinase (CK, EC 2.7.3.2) catalyzes the reversible phosphotransfer reaction between ATP/ADP and Cr/PCr. CK is proposed to be an “energy reservoir” that maintains intracellular ATP at a stable level and connects the different ATP subdomains in the excitable cells of higher vertebrates [23,24]. Two cytosolic isoforms with distinct tissue expression patterns have been identified for CK: the muscle-type (MMCK) and brain-type (BBCK) [25,26]. MMCK and BBCK are highly conserved in their sequence and share an almost superimposable tertiary structure [27]. The cytosolic CK exists as a dimer in solutions. Each subunit of CK is composed of two domains: a smaller N-terminal domain (NTD) containing only α -helices and a larger C-terminal domain (CTD) with both β -sheet and α -helix secondary structures (Figure 1). Since the first purification of rabbit muscle CK in 1954 [28], MMCK has been taken as a model enzyme and has been extensively studied in its structure, catalytic mechanism, physiological functions and folding, while only limited studies addressed the biophysical and biochemical properties of BBCK.

Figure 1. Structure of HBCK monomer (PDB ID: 3DRE) [27]. N and C denote the N- and C-terminus of the protein, respectively. The positions of the four Trp residues are highlighted by the space-filling model.



The folding mechanism of MMCK, when denatured or renatured in guanidine chloride or urea solutions, has been characterized as a multi-state process involving several intermediates [29-37]. Particularly, both kinetic and equilibrium folding studies have revealed the existence of a monomeric intermediate with unfolded NTD and folded CTD, and a dimeric inactive intermediate maintaining most of the native secondary structures. Both of these two intermediates are significantly disrupted at the tertiary structure level and are aggregation-prone, but the monomeric one is not accumulated during kinetic refolding [38]. The monomeric intermediate can be captured by the molecular chaperones GroEL and casein [39], while the dimeric intermediate can bind with the protein disulfide isomerase [38] and peptidyl-prolyl *cis-trans* isomerase [40].

The thermal denaturation of MMCK is dominated by a two-state irreversible process [41] with serious aggregation [42]. However, a pre-transitional conformational change in the CTD has been characterized by two-dimensional infrared spectroscopy and is proposed to be responsible for MMCK thermal aggregation [14]. The properties of the heat induced aggregation-prone state is similar to the dimeric inactivate intermediate that appeared during guanidine chloride denaturation, suggesting that the difference in the local stabilities of the CK molecule plays a crucial role in the onset of aggregation. However, no stable intermediate could be detected during the thermal denaturation of both rabbit and human MMCK [14,43].

Although MMCK and BBCK are highly similar in their structure and catalyze the same chemical reaction, isoenzyme-specific intracellular functions have been identified [44,45]. Recently, we also found that these two isoforms exhibit quite different properties during thermal inactivation [43]. The thermal stability of human MMCK (hMMCK) is much higher than that of human BBCK (hBBCK). The thermal inactivation of hMMCK is irreversible and is accompanied with serious aggregation, while that of hBBCK is partially reversible at temperatures below 55 °C. The distinct properties of these two isoenzymes suggest that they may undertake different structural changes during thermal denaturation. In this research, the sequential events in hBBCK thermal denaturation were investigated by spectroscopic methods.

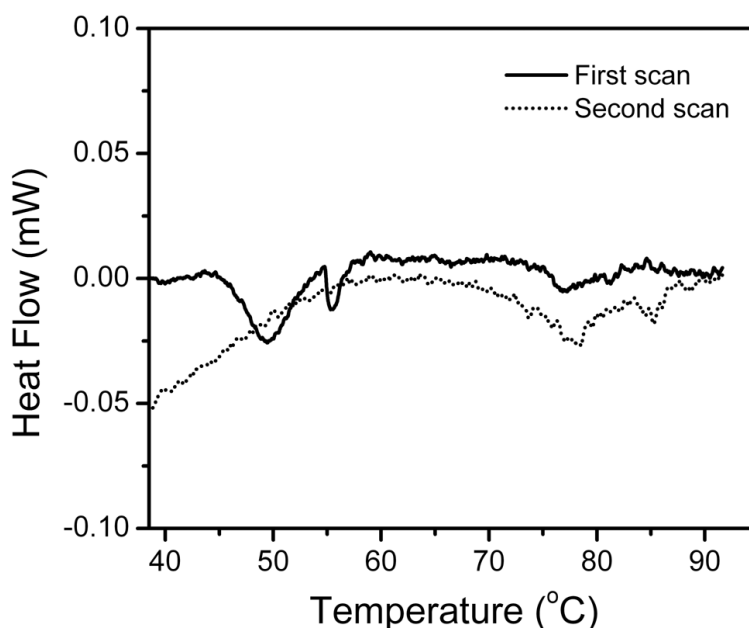
2. Results and Discussion

2.1. Thermal Denaturation of hBBCK Is Calorimetrically Irreversible

Our previous study has indicated that the thermal inactivation of hBBCK is partially reversible at temperatures below 55 °C, but no activity could be recovered by 24 h reactivation on ice for samples pre-heated at temperatures above 60 °C [43]. To elucidate whether the irreversibility was caused by the temperature-jump during cooling, differential scanning calorimetry (DSC) experiments were performed. As shown in Figure 2, the heat flow *versus* temperature profile contained several endothermic peaks, suggesting that the thermal denaturation of hBBCK contained stepwise transitions. The main peak was centered at about 50 °C, followed by a small peak at around 56 °C. At around 77 °C, there was an additional weak endothermic peak, which might be the further unfolding of the residual structures maintained in the non-native oligomers or small aggregates. It is noteworthy that no changes were observed in the turbidity of the solution when monitored by absorbance at 400 nm, even when the sample was heated up to 100 °C for 10 min, suggesting that the non-native oligomers

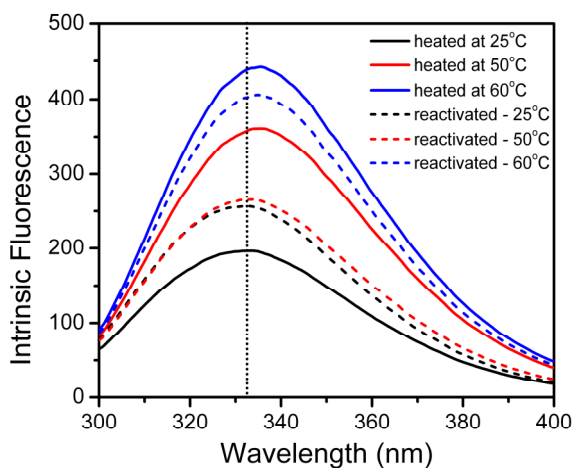
characterized in our previous study [43] did not associate into large amorphous aggregates at extremely high temperatures. This behavior is quite different from the thermal denaturation of MMCK [14,41,42]. The second scan was performed by heating the solutions up to 92 °C, cooling them at 20 °C, and reheating them to collect the calorimetric profile. No obvious thermal effect was observed in the area of the main endothermic peaks (45-60 °C) during the first scan, implying that the denaturation of hBBCK induced by heat was mainly dominated by a calorimetrically irreversible process. It is worth noting that several peaks and knobs appeared at high temperatures for the second scan, which might be due to the further unfolding of the residual structures or the partial reversibility of the transitions at high temperatures, or both.

Figure 2. Temperature dependence of the heat flow of hBBCK thermal denaturation monitored by DSC. The heating rate was 1 K/min. The protein concentration was 1 mg/mL. The first scan is shown by the solid line, and the dotted line represents the second scan, which was performed by reheating the samples after cooling from the first scan. The negative peaks in the DSC profile are endothermic.



To further study the reversibility of the hBBCK structure during thermal denaturation, intrinsic fluorescence spectra were collected for samples heated at a given temperature and reactivated on ice for 24 h. The typical spectra are presented in Figure 3. Since the intensity of the intrinsic fluorescence spectra of proteins is easily affected by many environmental factors, the maximum emission wavelength (E_{\max}) was used to reflect the structural integrity of the protein. After 24 h incubation, no significant change was observed in the E_{\max} value as well as the shape of the spectrum of the samples heated at 25 °C. For samples heated at 50 °C and 60 °C, the intrinsic fluorescence spectra had a red-shift of about 3 nm after being reactivated for 0 h. After 24 h of reactivation, the E_{\max} value of the sample pre-treated at 50 °C could recover to that of the native enzyme, whereas the sample pre-treated at 60 °C could not. These observations suggested that the irreversible inactivation of hBBCK at high temperatures observed in our previous research [43] was caused by the irreversible changes in hBBCK tertiary structure.

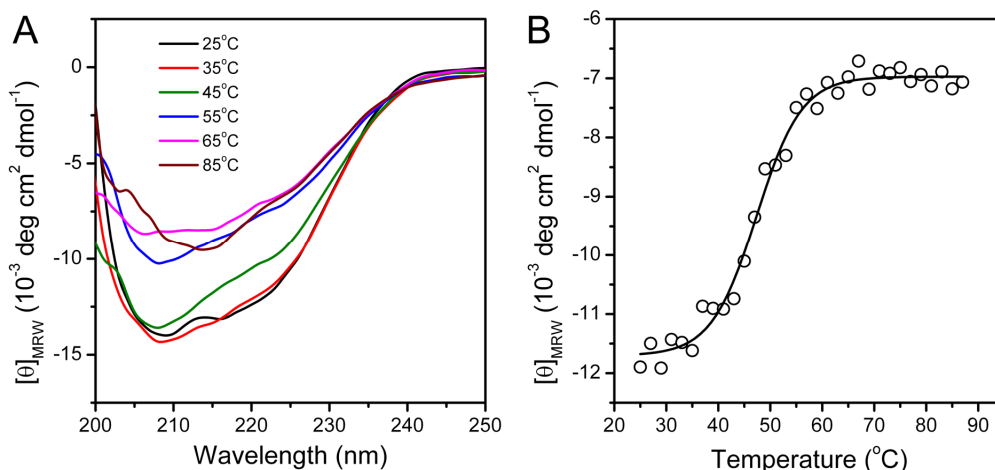
Figure 3. Intrinsic fluorescence spectra of the thermally inactivated and reactivated hBBCK samples. The inactivated samples were prepared by heating the enzyme solutions (0.2 mg/mL) at 25 °C, 50 °C, and 60 °C for 10 min, while the reactivated samples were prepared by incubating the inactivated samples on ice for 24 h. The intrinsic fluorescence was measured with an excitation wavelength of 280 nm.



2.2. hBBCK Thermal Denaturation Monitored by CD Spectroscopy

Far-UV CD spectroscopy is a sensitive monitor of changes in protein secondary structure [46]. The CD spectrum recorded at 25 °C exhibited a typical shape of $\alpha + \beta$ proteins (Figure 4), which is consistent with the structure of hBBCK shown in Figure 1. At high temperatures, the shape of the CD spectra revealed that denatured protein was dominated by β -sheet structures and lacked helical structures. This was reflected by the single negative peak at around 215 nm. The change in the CD data was best-fitted by a two-state process, and the midpoint temperature of transition (T_m) was 47.3 ± 0.4 °C.

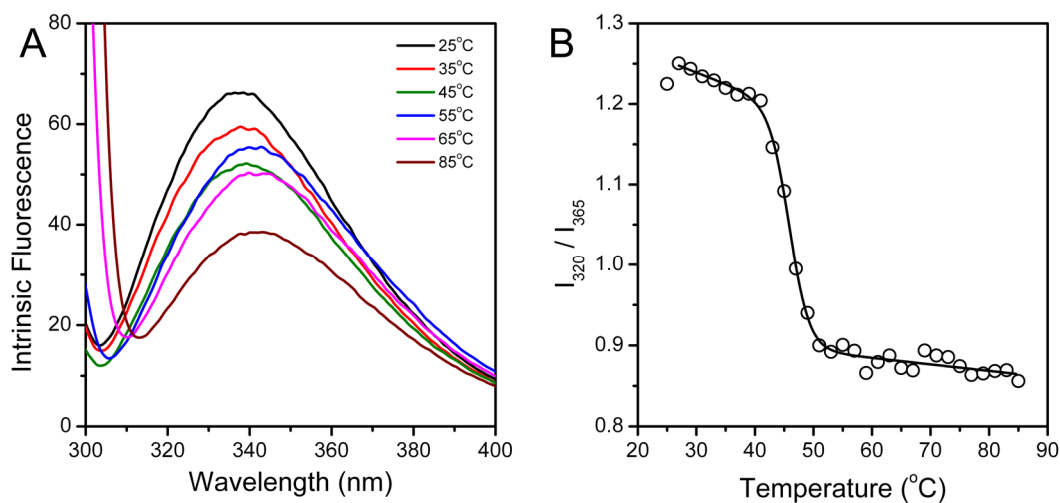
Figure 4. hBBCK thermal denaturation monitored by CD spectroscopy. (A) Typical CD spectra of hBBCK recorded at a given temperature after 2 min equilibration. (B) Changes in the ellipticity at 222 nm with the increase of temperature. The CD data are presented as mean residue molar ellipticity ($[\theta]_{MRW}$).



2.3. hBBCK Thermal Denaturation Monitored by Intrinsic Fluorescence Spectroscopy

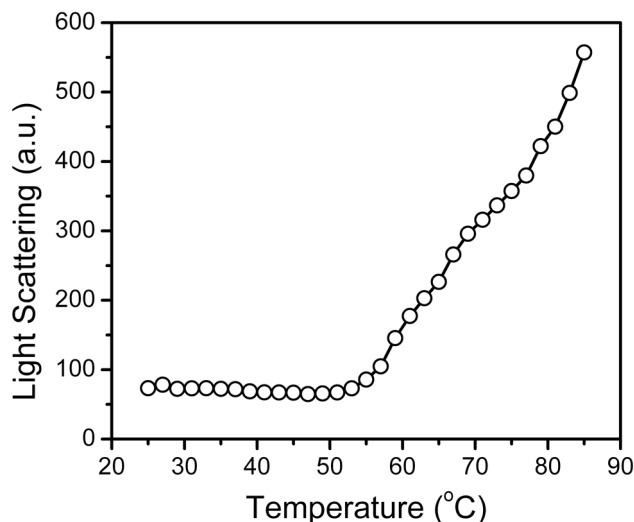
hBBCK contains four Trp residues located in the CTD (Figure 1), while the Tyr residues are distributed in both the NTD and the CTD. To probe the tertiary structural changes of hBBCK during thermal denaturation, intrinsic fluorescence were measured using an excitation wavelength of both 280 nm and 295 nm. When excited at 280 nm, the fluorescence is from the contributions of both Trp and Tyr, while only the Trp fluorophores are detected when excited at 295 nm. No significant difference in the transition curves was observed by the two excitation wavelengths, and thus the spectra excited at 295 nm were used for further analysis. As shown in Figure 5A, the Trp fluorescence had a slight red-shift (~ 5 nm) during thermal denaturation. The relative small change made it difficult to measure the E_{\max} value precisely. Thus I_{320}/I_{365} , which is a measure of the spectral shape [47], was used to reflect the change in the Trp fluorescence spectra during heating. The I_{320}/I_{365} value decreased slightly when the temperature increased from 25 °C to 40 °C, suggesting that the fluorophores had become more water-accessible during heating. The main transition occurred in the temperature range of 41–51 °C with a T_m value of 45.7 ± 0.2 °C.

Figure 5. hBBCK thermal denaturation monitored by intrinsic fluorescence spectroscopy excited at 295 nm. **(A)** Fluorescence spectra of hBBCK recorded at the given temperature after 2 min equilibration. **(B)** Dependence of I_{320}/I_{365} on temperature.



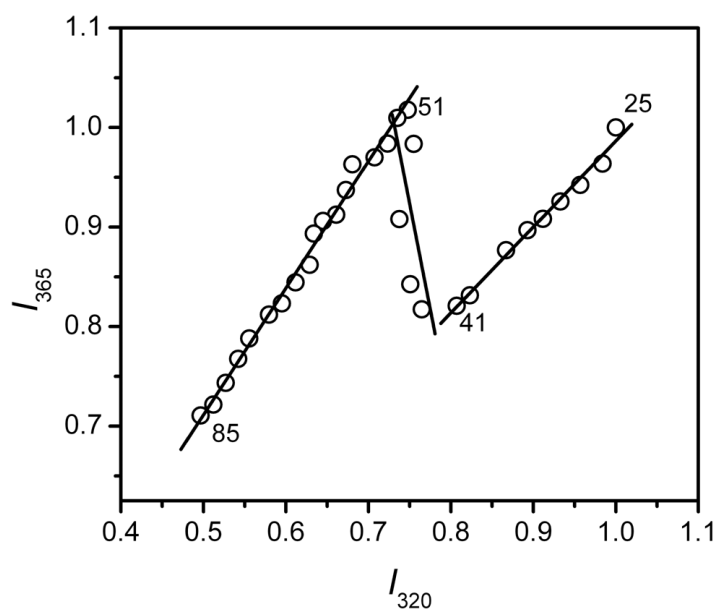
During thermal denaturation, hBBCK is prone to form large aggregates that are easily detected by turbidity measurements. Our previous study indicated that hBBCK only formed non-native oligomers or small aggregates that could not be detected by turbidity experiments. However, these aggregates are visible in the size-exclusion chromatography when quenched on ice. To monitor the formation of the oligomers during the heating process, resonance Rayleigh light scattering was monitored as a function of temperature (Figure 6). No significant changes in the light scattering occurred at temperatures below 51 °C, followed by a continuous increase for temperatures higher than 51 °C. Two transitions could be distinguished, as seen in Figure 6, with temperatures ranging from 51 °C to 77 °C and >77 °C, respectively. These transitions coincided with the existence of additional endothermic peaks at around 77 °C in the DSC profile (Figure 2).

Figure 6. Changes in the oligomeric states during hBBCK thermal denaturation monitored by resonance light scattering.



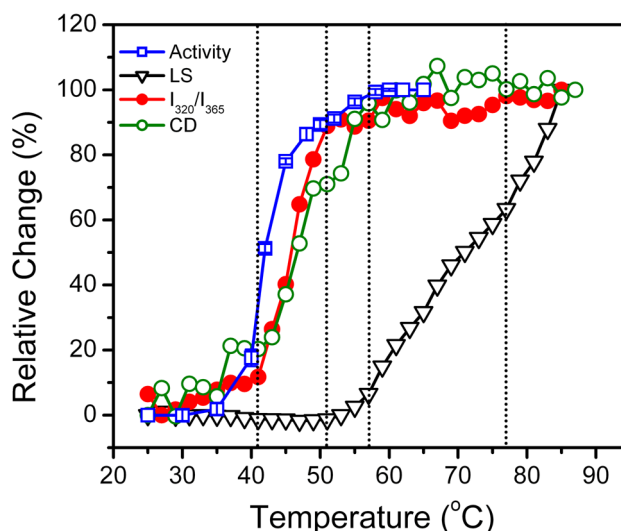
The T_m value from intrinsic fluorescence was about 1.5 °C smaller than that from CD spectroscopy, suggesting that the changes in hBBCK secondary and tertiary structures were not synchronous. To further probe the stepwise changes in hBBCK thermal denaturation, a phase diagram was constructed to detect the asynchronous changes of the hydrophobic (monitored by I_{320}) and hydrophilic fluorophores (monitored by I_{365}). The diagram of hBBCK thermal denaturation was composed of three linear parts with joint positions at 41 °C and 51 °C, respectively (Figure 7). In the phase diagram, each straight line represents a two-state process, and the joint position indicates the appearance of a possible intermediate [48]. Thus, the results in Figure 7 indicated that the microenvironmental changes of hBBCK Trp residues induced by heat involved at least three distinct transitions.

Figure 7. Phase diagram analysis of the fluorescence data shown in Figure 5. The diagram was constructed by plotting I_{320} versus I_{365} . The I_{320} and I_{365} values were normalized by the maximum value in each set of the fluorescence data.



The above results from spectroscopic analysis clearly indicated that the thermal denaturation of hBBCK was a stepwise process. A summary of the transition curves is presented in Figure 8. When temperature increased from room temperature to body temperature, no significant change was observed in hBBCK secondary structures. However, a minor increase was observed in the solvent exposure of the Trp fluorophores, which might reflect the increase of structural fluctuations that correspond with the increase of temperature. The enzyme began to lose its activity from 41 °C. This loss of activity was accompanied by significant structural changes at both the secondary and tertiary structure levels. The activity loss occurred prior to the structural transitions, suggesting that the modification of the active site structure proceeded from the unfolding of the overall structure. At 51 °C, hBBCK lost most of its activity and the changes in the microenvironments of the Trp fluorophores was finished, while a further decrease was found in the hBBCK regular secondary structures at temperatures above 51 °C. These asynchronous structural transitions might be the reason why two endothermic peaks were observed in the DSC profile within the temperature range of 40-60 °C. At temperatures above 55 °C, the unfolded molecules began to associate into non-native oligomers. An increase in either the associating rate or the size of the oligomers occurred at 77 °C, which was confirmed by the appearance of an additional endothermic peak centered at around 77 °C in the DSC profile. These sequential events were quite different from those of MMCK [14]. As for MMCK, the unfolding of native structures is closely correlated to thermal aggregation. In contrast to MMCK, the unfolding and aggregation were sequential or separated events for hBBCK. These results also suggested that the isoenzymes had differential local stabilities in their structure, which might contribute to the discrepancy in their thermal stabilities.

Figure 8. A summary of the transition curves obtained by various probes. The activity data were from [43].



It is worth noting that both hMMCK and hBBCK were not fully unfolded during thermal denaturation. The changes of the E_{\max} values, in particular, were minor for both proteins when compared to the chemical denaturants-induced unfolding. When denatured by guanidine chloride, the E_{\max} of the fully unfolded state is at about 350 nm [32,49-51], which reflects that all of the Trp fluorophores are fully exposed to the solvent. However, the E_{\max} of the thermally denatured state was at around 342 nm, implying that most of the fluorophores had limited solvent accessibility. These

observations are consistent with the proposal that protein thermal aggregation involves the exposure of certain regions and does not require the protein to be fully unfolded [20].

3. Experimental Section

3.1. Materials

Sodium dodecylsulfate (SDS), isopropyl-1-thio- β -D-galactopyranoside (IPTG), Tris, creatine, ATP, DTT, and thymol blue were purchased from Sigma. All the other reagents were local products of analytical grade.

3.2. Protein Expression and Purification

Recombinant hBBCK was overexpressed in *Escherichia coli* BL21 [DE3]-pLysS (Stratagene, Germany) and purified as described previously [43,51]. The final products were collected from a Sephacryl S300 HR column equipped on an ÄKTA purifier. The protein concentration was determined according to the Bradford method by using bovine serum albumin as a standard [52]. All enzyme solutions were prepared by dissolving the proteins in 10 mM Tris-HCl at a pH of 8.0.

3.3. Activity Assay

CK activity was measured according to the pH-colorimetry method [29] in the phosphocreatine formation direction by monitoring the absorbance changes at 597 nm on an Ultraspec-4300 Pro spectrophotometer. All the activity experiments were performed at 25 °C and repeated for at least three times. The thermal inactivated and reactivated samples were prepared using the sample procedures as described previously [43].

3.4. DSC Experiments

DSC experiments were performed using a Setaram Micro DSC III calorimeter. The final protein concentration was 1 mg/mL for the DSC experiments, and the solution volume was 0.8 mL. The DSC profiles were obtained using a scan rate of 1 K/min from 20 °C to 92 °C. The second scan was carried out by reheating the samples after they were cooled to 20 °C and equilibrated for 30-40 min.

3.5. Spectroscopy

All resultant spectra were obtained by the subtraction of the control. Far-UV circular dichroism (CD) spectra were recorded on a Jasco-715 spectrophotometer using a cell with a path length of 0.1 cm. The formation of the non-native oligomers was monitored by measuring the resonance light scattering at 90° using Trp as the intrinsic fluorophore excited at 295 nm [53]. Intrinsic fluorescence spectra were measured on a Hitachi F2500 or F4500 spectrophotometer with an excitation wavelength of 280 nm (to excite both Trp and Tyr) or 295 nm (to excite Trp only). The phase diagram of the fluorescence data was constructed using the published procedure [48]. In brief, the fluorescence intensity at 320 nm (I_{320}) and 365 nm (I_{365}) were normalized by the maximum of each data set, and then the diagram was constructed by plotting I_{320} versus I_{365} .

4. Conclusions

In this research, the sequential events in hBBCK thermal denaturation were studied by DSC, CD, and intrinsic fluorescence spectroscopy. The DSC results indicated that the thermal denaturation of hBBCK was calorimetrically irreversible. The discrepancy in the transition curves obtained from various probes suggested that hBBCK undergo sequential structural changes when subjected to thermal stress. During heating, the disruption of the active site structure occurred prior to the secondary and tertiary structural changes. The thermal unfolding and aggregation of hBBCK was found to occur via sequential events, which is quite different from that of MMCK. The results herein suggested that hBBCK and hMMCK undergo quite dissimilar thermal unfolding pathways, although they are highly conserved in their primary and tertiary structures. The minor difference in structure might endow the isoenzymes dissimilar local stabilities in structure, which further contribute to the isoenzyme-specific thermal stabilities.

Acknowledgements

This investigation was supported by the National Natural Science Foundation of China (No. 30970559).

References

1. Jaenicke, R. Stability and folding of domain proteins. *Prog. Biophys. Mol. Biol.* **1999**, *71*, 155-241.
2. Jaenicke, R.; Lilie, H.; Matthews, C.R. Folding and association of oligomeric and multimeric proteins. *Adv. Protein Chem.* **2000**, *53*, 329-362.
3. Burgess, A.W.; Scheraga, H.A. A hypothesis for the pathway of the thermally-induced unfolding of bovine pancreatic ribonuclease. *J. Theor. Biol.* **1975**, *53*, 403-420.
4. Matheson, R.R., Jr.; Scheraga, H.A. Steps in the pathway of the thermal unfolding of ribonuclease A. A nonspecific photochemical surface-labeling study. *Biochemistry* **1979**, *18*, 2437-2445.
5. Matheson, R.R., Jr.; Scheraga, H.A. Steady-state kinetic study of action of ribonuclease A, involving a conformational change between 30 and 40 degrees C. *Biochemistry* **1979**, *18*, 2446-2450.
6. Navon, A.; Ittah, V.; Laity, J.H.; Scheraga, H.A.; Haas, E.; Gussakovsky, E.E. Local and long-range interactions in the thermal unfolding transition of bovine pancreatic ribonuclease A. *Biochemistry* **2001**, *40*, 93-104.
7. Stelea, S.D.; Keiderling, T.A. Pretransitional structural changes in the thermal denaturation of ribonuclease S and S protein. *Biophys. J.* **2002**, *83*, 2259-2269.
8. Stelea, S.D.; Pancoska, P.; Benight, A.S.; Keiderling, T.A. Thermal unfolding of ribonuclease A in phosphate at neutral pH: Deviations from the two-state model. *Protein Sci.* **2001**, *10*, 970-978.
9. Vermeer, A.W.; Norde, W. The thermal stability of immunoglobulin: Unfolding and aggregation of a multi-domain protein. *Biophys. J.* **2000**, *78*, 394-404.

10. Paquet, M.J.; Laviolette, M.; Pezolet, M.; Auger, M. Two-dimensional infrared correlation spectroscopy study of the aggregation of cytochrome c in the presence of dimyristoylphosphatidylglycerol. *Biophys. J.* **2001**, *81*, 305-312.
11. Dong, A.; Randolph, T.W.; Carpenter, J.F. Entrapping intermediates of thermal aggregation in a-helical proteins with low concentration of guanidine hydrochloride. *J. Biol. Chem.* **2000**, *275*, 27689-27693.
12. Fabian, H.; Mantsch, H.H.; Schultz, C.P. Two-dimensional IR correlation spectroscopy: Sequential events in the unfolding process of the *l* cro-V55C repressor protein. *Proc. Natl. Acad. Sci. USA* **1999**, *96*, 13153-13158.
13. Yan, Y.-B.; Wang, Q.; He, H.-W.; Hu, X.-Y.; Zhang, R.-Q.; Zhou, H.-M. Two-dimensional infrared correlation spectroscopy study of sequential events in the heat-induced unfolding and aggregation process of myoglobin. *Biophys. J.* **2003**, *85*, 1959-1967.
14. He, H.-W.; Zhang, J.; Zhou, H.-M.; Yan, Y.-B. Conformational change in the C-terminal domain is responsible for the initiation of creatine kinase thermal aggregation. *Biophys. J.* **2005**, *89*, 2650-2658.
15. Zhang, J.; Yan, Y.-B. Probing conformational changes of proteins by quantitative second-derivative infrared spectroscopy. *Anal. Biochem.* **2005**, *340*, 89-98.
16. Yan, Y.-B.; Zhang, J.; He, H.-W.; Zhou, H.-M. Oligomerization and aggregation of bovine pancreatic ribonuclease A: Characteristic events observed by FTIR spectroscopy. *Biophys. J.* **2006**, *90*, 2525-2533.
17. Zhang, J.; He, H.-W.; Wang, Q.; Yan, Y.-B. Sequential events in ribonuclease A thermal unfolding characterized by two-dimensional infrared correlation spectroscopy. *Protein Pep. Lett.* **2006**, *13*, 33-40.
18. Su, J.-T.; Kim, S.-H.; Yan, Y.-B. Dissecting the pretransitional conformational changes in aminoacylase I thermal denaturation. *Biophys. J.* **2007**, *92*, 578-587.
19. Stadler, A.M.; Digel, I.; Artmann, G.M.; Embs, J.P.; Zaccari, G.; Buldt, G. Hemoglobin dynamics in red blood cells: Correlation to body temperature. *Biophys. J.* **2008**, *95*, 5449-5461.
20. Yan, Y.-B.; Wang, Q.; He, H.-W.; Zhou, H.-M. Protein thermal aggregation involves distinct regions: Sequential events in the heat-induced unfolding and aggregation of hemoglobin. *Biophys. J.* **2004**, *86*, 1682-1690.
21. Digel, I.; Maggakis-Kelemen, C.; Zerlin, K.F.; Linder, P.; Kasischke, N.; Kayser, P.; Porst, D.; Artmann, A.T.; Artmann, G.M. Body temperature-related structural transitions of monotremal and human hemoglobin. *Biophys. J.* **2006**, *91*, 3014-3021.
22. Zerlin, K.F.T.; Kasischke, N.; Digel, I.; Maggakis-Kelemen, C.; Artmann, A.T.; Porst, D.; Kayser, P.; Linder, P.; Artmann, G.M. Structural transition temperature of hemoglobins correlates with species' body temperature. *Eur. Biophys. J.* **2007**, *37*, 1-10.
23. Wallimann, T.; Wyss, M.; Brdiczka, D.; Nicolay, K.; Eppenberger, H.M. Intracellular compartmentation, structure and function of creatine kinase isoenzymes in tissues with high and fluctuating energy demands: The 'phosphocreatine circuit' for cellular energy homeostasis. *Biochem. J.* **1992**, *281*, 21-40.
24. Wallimann, T. Bioenergetics: Dissecting the role of creatine kinase. *Curr. Biol.* **1994**, *4*, 42-46.

25. Wallimann, T.; Hemmer, W. Creatine-kinase in nonmuscle tissues and cells. *Mol. Cell. Biochem.* **1994**, *133*, 193-220.
26. McLeish, M.J.; Kenyon, G.L. Relating structure to mechanism in creatine kinase. *Crit. Rev. Biochem. Mol. Biol.* **2005**, *40*, 1-20.
27. Bong, S.M.; Moon, J.H.; Nam, K.H.; Lee, K.S.; Chi, Y.M.; Hwang, K.Y. Structural studies of human brain-type creatine kinase complexed with the ADP-Mg²⁺-NO₃-creatine transition-state analogue complex. *FEBS Lett.* **2008**, *582*, 3959-3965.
28. Kuby, S.A.; Noda, L.; Lardy, H.A. Adenosinetriphosphate-creatine transphosphorylase. I. Isolation of the crystalline enzyme from rabbit muscle. *J. Biol. Chem.* **1954**, *209*, 191-201.
29. Yao, Q.Z.; Zhou, H.M.; Hou, L.X.; Zou, C.G. A comparison of denaturation and inactivation rates of creatine kinase in guanidine solutions. *Sci. Sin. B* **1982**, *25*, 1296-1802.
30. Morris, G.E.; Frost, L.C.; Newport, P.A.; Hudson, N. Monoclonal antibody studies of creatine kinase: Antibody-binding sites in the N-terminal region of creatine kinase and effects of antibody on enzyme refolding. *Biochem. J.* **1987**, *248*, 53-59.
31. Webb, T.; Jackson, P.J.; Morris, G.E. Protease digestion studies of an equilibrium intermediate in the unfolding of creatine kinase. *Biochem. J.* **1997**, *321*, 83-88.
32. Fan, Y.X.; Zhou, J.M.; Kihara, H.; Tsou, C.L. Unfolding and refolding of dimeric creatine kinase equilibrium and kinetic studies. *Protein Sci.* **1998**, *7*, 2631-2641.
33. Leydier, C.; Clottes, E.; Couthon, F.; Marcillat, O.; Ebel, C.; Vial, C. Evidence for kinetic intermediate states during the refolding of GdnHCl-denatured MM-creatine kinase. Characterization of a trapped monomeric species. *Biochemistry* **1998**, *37*, 17579-17589.
34. Li, S.; Bai, J.H.; Park, Y.D.; Zhou, H.M. Aggregation of creatine kinase during refolding and chaperonin-mediated folding of creatine kinase. *Int. J. Biochem.: Cell Biol.* **2001**, *33*, 279-286.
35. Park, Y.D.; Ou, W.B.; Yu, T.W.; Zhou, H.M. Folding pathway for partially folded rabbit muscle creatine kinase. *Biochem. Cell Biol.* **2001**, *79*, 479-487.
36. Mazon, H.; Marcillat, O.; Vial, C.; Clottes, E. Role of C-terminal sequences in the folding of muscle creatine kinase. *Biochemistry* **2002**, *41*, 9646-9653.
37. Mazon, H.; Marcillat, O.; Forest, E.; Smith, D.L.; Vial, C. Conformational dynamics of the GdmHCl-induced molten globule state of creatine kinase monitored by hydrogen exchange and mass spectrometry. *Biochemistry* **2004**, *43*, 5045-5054.
38. Zhao, T.J.; Ou, W.B.; Xie, Q.; Liu, Y.; Yan, Y.B.; Zhou, H.M. Catalysis of creatine kinase refolding by protein disulfide isomerase involves disulfide cross-link and dimer to tetramer switch. *J. Biol. Chem.* **2005**, *280*, 13470-13476.
39. Li, S.; Bai, J.H.; Park, Y.D.; Zhou, H.M. Capture of monomeric refolding intermediate of human muscle creatine kinase. *Protein Sci.* **2006**, *15*, 171-181.
40. Ou, W.B.; Luo, W.; Park, Y.D.; Zhou, H.M. Chaperone-like activity of peptidyl-prolyl *cis-trans* isomerase during creatine kinase refolding. *Protein Sci.* **2001**, *10*, 2346-2353.
41. Lyubarev, A.E.; Kurganov, B.I.; Orlov, V.N.; Zhou, H.M. Two-state irreversible thermal denaturation of muscle creatine kinase. *Biophys. Chem.* **1999**, *79*, 199-204.

42. Meng, F.G.; Hong, Y.K.; He, H.W.; Lyubarev, A.E.; Kurganov, B.I.; Yan, Y.B.; Zhou, H.M. Osmophobic effect of glycerol on irreversible thermal denaturation of rabbit creatine kinase. *Biophys. J.* **2004**, *87*, 2247-2254.
43. Gao, Y.-S.; Zhao, T.-J.; Chen, Z.; Li, C.; Wang, Y.; Yan, Y.-B.; Zhou, H.-M. Isoenzyme-specific thermostability of human cytosolic creatine kinase. *Int. J. Biol. Macromol.* **2010**, *47*, 27-32.
44. Wallimann, T.; Moser, H.; Eppenberger, H.M. Isozyme-specific localization of M-line bound creatine kinase in myogenic cells. *J. Muscle Res. Cell Motil.* **1983**, *4*, 429-441.
45. Hornemann, T.; Stolz, M.; Wallimann, T. Isoenzyme-specific interaction of muscle-type creatine kinase with the sarcomeric M-line is mediated by NH₂-terminal lysine charge-clamps. *J. Cell Biol.* **2000**, *149*, 1225-1234.
46. Pelton, J.T.; McLean, L.R. Spectroscopic methods for analysis of protein secondary structure. *Anal. Biochem.* **2000**, *277*, 167-176.
47. Turoverov, K.K.; Haitlina, S.Y.; Pinaev, G.P. Ultra-violet fluorescence of actin. Determination of native actin content in actin preparations. *FEBS Lett.* **1976**, *62*, 4-6.
48. Bushmarina, N.A.; Kuznetsova, I.M.; Biktashev, A.G.; Turoverov, K.K.; Uversky, V.N. Partially folded conformations in the folding pathway of bovine carbonic anhydrase II: A fluorescence spectroscopic analysis. *ChemBioChem* **2001**, *2*, 813-821.
49. Feng, S.; Xu, Z.; Yan, Y.-B. Blocking creatine kinase refolding by trace amounts of copper ions. *J. Inorg. Biochem.* **2008**, *102*, 928-935.
50. He, H.-W.; Feng, S.; Pang, M.; Zhou, H.-M.; Yan, Y.-B. Role of the linker between the N- and C-terminal domains in the stability and folding of rabbit muscle creatine kinase. *Int. J. Biochem. Cell Biol.* **2007**, *39*, 1816-1827.
51. Zhao, T.-J.; Feng, S.; Wang, Y.-L.; Liu, Y.; Luo, X.-C.; Zhou, H.-M.; Yan, Y.-B. Impact of intra-subunit domain-domain interactions on creatine kinase activity and stability. *FEBS Lett.* **2006**, *580*, 3835-3840.
52. Bradford, M.M. A rapid and sensitive method for the quantitation of microgram quantities of protein utilizing the principle of protein-dye binding. *Anal. Biochem.* **1976**, *72*, 248-254.
53. He, G.-J.; Zhang, A.; Liu, W.-F.; Cheng, Y.; Yan, Y.-B. Conformational stability and multistate unfolding of poly(A)-specific ribonuclease. *FEBS J.* **2009**, *276*, 2849-2860.